BUTTERWORTH HEINEMANN

Polymer Vol. 36 No. 4, pp. 719–724, 1995

0032-3861/95/$10.00 + 0.00

Photoionization of donor–acceptor complex by the internal electric field in blend of poly(vinylidene fluoride) and poly(methyl methacrylate)

Naoto Tsutsumi*, Ichiro Fujii and Tsuyoshi Kiyotsukuri
Department of Polymer Science and Engineering, Kyoto Institute of Technology, Matsugasaki, Sakyoku, Kyoto 606, Japan
(Received 18 March 1994; revised 25 May 1994)

This paper presents a measurement of the photocurrent of a poled blend of 80 wt% poly(vinylidene fluoride) (PVDF) and 20 wt% poly(methyl methacrylate) (PMMA) containing 5 wt% *N*-phenylcarbazole (PhCz) and 1 wt% 2,4,7-trinitro-9-fluorenone (TNF) molecules and a discussion of the photoionization of the PhCz–TNF complex by the internal electric field. The high internal electric field, of the order of 10^6 V cm^{-1}, created by the preferential orientation of polar PVDF β crystallites assists the photoionization of an ion-pair in the polymer matrix, and thus free photocarrier formation by the internal electric field can be expected. The photocurrent illuminated from the positive poled side corresponds to the absorption spectrum of PhCz, while the photocurrent from the negative poled side has maximum current in the absorption edge of PhCz and no photocurrent activity in the strong absorption region of PhCz below 330 nm. No photocurrent was measured for the unpoled sample. These results imply that the internal electric field induced by poling has a significant role in carrier photogeneration. Furthermore, the optical absorbance due to the charge-transfer complex between PhCz and TNF increased non-linearly with increasing poling field.

(Keywords: photoionization; donor–acceptor complex; PVDF/PMMA blend)

INTRODUCTION

Poly(vinylidene fluoride) (PVDF) and poly(methyl methacrylate) (PMMA) form compatible blends in all proportions in the molten state[1]. When a blend with PVDF content greater than 50 wt% is cooled from the melt[1], part of the PVDF component crystallizes as a separate phase. The remaining amorphous material is a compatible blend of the two polymers with a single glass transition temperature (T_g) intermediate between those of the two components[1]. Fourier-transform infra-red spectroscopy of PVDF/PMMA has shown that the 70/30 wt% composition crystallizes in the β-crystal form of PVDF when the blend is quenched from the melt[2]. A separate study of an 80/20 wt% PVDF/PMMA blend revealed that this composition, when melt-quenched, also crystallizes preferentially in the β phase and that the β fraction increases when the sample is annealed at a temperature of approximately 120°C[3].

Tsutsumi *et al.* have already reported the internal electric field created by the preferentially oriented polar β crystals in a copolymer of vinylidene fluoride and trifluoroethylene (P(VDF–TrFE))[4], in a melt-quenched and subsequently annealed blend of 80 wt% PVDF and 20 wt% PMMA[5,6] and in blends of P(VDF–TrFE) and PMMA[7], using the spectral shift of an electrochromic dye dissolved in the amorphous region of the polymer matrix. Well poled films have an internal electric field in the range of (2–4) × 10^6 V cm^{-1}, which is approximately three or four times larger than the poling field. When dye molecules, which have non-linear optical (NLO) properties, are dispersed poled PVDF/PMMA blend films exhibit second-harmonic generation arising from the NLO molecules oriented by the internal electric field[8].

We think that the internal electric field created by the oriented polar PVDF β crystals will be high enough to photoionize ion-pairs in the polymer matrix, and thus free photocarrier formation by the internal electric field can be expected. To confirm this new idea, in this study we have measured the photocurrent for the poled PVDF/PMMA (80/20 wt%) blend containing *N*-phenylcarbazole (PhCz) as an electron donor and 2,4,7-trinitro-9-fluorenone (TNF) as an electron acceptor, and investigated the possibility of carrier photogeneration by the internal electric field induced by poling.

EXPERIMENTAL

Sample preparation

PVDF (Kureha, KF-polymer, $M_w = 141\,000$, $M_n = 64\,000$) and PMMA (Mitsubishi Rayon, Acrypett-VHK, $M_w = 168\,000$, $M_n = 96\,400$) were used. PHCz and TNF were used as received. 4-Dimethylamino-4′-nitrostilbene (DANS), an electrochromic probe dye for internal electric field calculation, was recrystallized from amyl

* To whom correspondence should be addressed

alcohol solution. *N,N*-Dimethylacetamide solution of the blend polymer of PVDF/PMMA (80/20 wt%) with 5 wt% PhCz and 1 wt% TNF was cast to obtain films. After drying the cast films, they were melt-pressed between 50 μm thick films of Upilex (Ube Industry) on a heated press to a thickness between 40 and 60 μm. Then the molten films were quenched into liquid nitrogen and annealed at 120°C for 2 h before poling.

Electrical and optical measurements

The blend films were poled by applying a constant field between 0.1 and 0.8 MV cm^{-1} for 1 h at 80°C in nitrogen atmosphere to aluminium electrodes that had been evaporated onto opposing surfaces of the films. The pyroelectric coefficient C_{pyro} was determined by measuring the current generated upon heating and cooling the poled film at a measured rate, usually ca. 0.6°C min^{-1} in the vicinity of 30°C. Ultra-violet/visible spectra of the samples were measured on a Shimadzu model UV-2101PC spectrophotometer controlled by PC microcomputer.

Figure 1 shows the schematic diagram for measuring the photocurrent. When the photocurrent is measured, one aluminium electrode was replaced by an indium tin oxide (ITO) quartz electrode after removing that aluminium electrode using 0.1 N sodium hydroxide solution. When the photocurrent is measured with no external electric field, ITO glass was grounded. The power supply (P.S. in *Figure 1*) was used to apply the external electric field. The photocurrent was determined by measuring the current that flows in the external resistance R_S, using a Takeda Riken model TR-84M electrometer, when the sample film was illuminated by monochromatic xenon light. The xenon light (Hamamatsu model L2274-01) was monochromated using a Ritsu Oyo Kougaku model MC-10N monochromator. The dark current was measured without illumination.

Characterization

Wide-angle X-ray scattering (WAXS) of the films was measured using a Toshiba model ADG-301 X-ray diffractometer with nickel-filtered Cu Kα radiation.

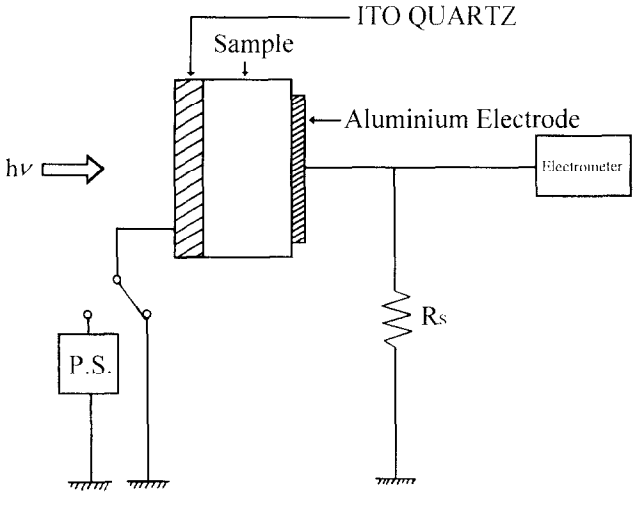

Figure 1 Schematic diagram of photocurrent measurement (P.S. is power supply)

Differential scanning calorimetry (d.s.c.) was performed at a heating rate of 10°C min^{-1} in nitrogen atmosphere, using a Perkin–Elmer model DSC 7 controlled by a 1020 TA workstation.

BASIS FOR MEASUREMENT OF INTERNAL ELECTRIC FIELD

Internal electric field E_i was determined by the electrochromic spectral shift of the probe molecule DANS in the polymer matrix. A theory for electrochromic effects in liquid solutions was developed and published by Liptay and co-workers in a series of papers, which are well summarized in the chapter of a book[9]. The theory was applied to electrochromic molecules dissolved in a polymer matrix by Havinga and van Pelt[10]. Furthermore, Tsutsumi *et al.* applied the equations developed by Havinga and van Pelt to the internal electric field calculation[4]. The detailed procedure for deriving the equations is summarized in ref. 4. The final form of the equation:

$$\frac{1}{(1-f)[1-G(u)]}\frac{A(\nu,E)}{\nu}-\frac{A(\nu,0)}{\nu} = \frac{G(u)}{[1-G(u)]^2}\left(-3C\frac{\partial}{\partial\nu}\frac{A(\nu,0)}{\nu}+\frac{3}{2}C^2\frac{\partial^2}{\partial\nu^2}\frac{A(\nu,0)}{\nu}\right) \quad (1)$$

was used to determine E_i, where $A(\nu,0)$ and $A(\nu,E)$ are, respectively, the absorbance of DANS in the presence and absence of field E at optical frequency ν, f is a factor expressing a wavelength-independent absorbance reduction from sources other than the electric field[4], and:

$$G(u)=1-\frac{3\coth(u)}{u}+\frac{3}{u^2} \quad (2)$$

$$u=\frac{E_i\mu_g}{kT} \quad (3)$$

$$C=\frac{kT\Delta\mu}{hc\mu_g} \quad (4)$$

where μ_g is the dipole moment of DANS in the ground state, k is Boltzmann's constant, T is absolute temperature, $\Delta\mu$ is the difference between the dipole moments in the excited and ground states ($=\mu_g-\mu_e$), h is Planck's constant and c is the speed of light.

The spectrum after poling, reduced from the original by factors f and $G(u)$, will cross the original spectrum at some value of wavenumber ν_N, where

$$A(\nu_N,E)/\{(1-f)[1-G(u)]\nu_N\}=A(\nu_N,0)/\nu_N$$

At the intersection, the right-hand side of equation (1) will be equal to zero, from which it can be deduced that

$$\partial[A(\nu,0)/\nu]/\partial\nu=(C/2)\partial^2[A(\nu,0)/\nu]/\partial\nu^2$$

First and second derivatives of $A(\nu,0)/\nu$ are evaluated as a function of ν to determine the value ν_N for which the above relation was satisfied. A value of $(1-f)[1-G(u)]$ was then chosen to make the spectra of the poled and unpoled samples intersect at ν_N, i.e.

$$A(\nu_N,E)/\{(1-f)[1-G(u)]\nu_N\}=A(\nu_N,0)/\nu_N$$

Having normalized the curves at ν_N, the difference in absorbance between the two spectra at several other

values of v are then determined, the derivatives are evaluated at the corresponding values of v as required for equation (1) and the quantity $\{G(u)/[1-G(u)]^2\}$ is evaluated from a linear least-squares fit. From $G(u)$ and equation (2), a value of u is obtained from which E_i is evaluated with $\mu_g = 7.4$ D, $\mu_e = 24.8$ D and $\Delta\mu = 17.4$ D for the DANS molecule[11,12].

RESULTS AND DISCUSSION

Polymer structure

Figure 2 shows WAXS results in the form of diffracted intensity *versus* scattering angle (2θ scan) for the samples with 5 wt% PhCz and 1 wt% TNF melt-quenched, thermally annealed at 120°C for 2 h and successively poled under 0.5 MV cm^{-1} at 80°C for 30 min. Peaks at 20.8°, 36.6° and 41.2° correspond to those of the β-crystal form[13]. The β peaks that are already perceptible in the melt-quenched blend scan intensify on annealing and successive poling. Preferential alignment of β crystallites by poling permits further crystallization. *Figure* 3 shows the d.s.c. thermogram for the corresponding samples. The endothermic peaks due to the melting of β crystal and α crystal appear at 160 and 172°C, respectively. The melting of β-crystal phase is followed by recrystallization to form α-crystal phase. The endothermic peak at 133°C for the annealed sample may be ascribed to thermodynamic relaxation, and this peak temperature depends on the annealing temperature before d.s.c. measurement.

Photocurrent

Figure 4 exhibits the time–current profile when the sample is illuminated by monochromatic light without applying any external electric field. The current that flowed when the positive poled side is grounded is referred to as i_d^+ and i_p^+, where subscripts d and p mean current flow in the dark and on photo-illumination, respectively.

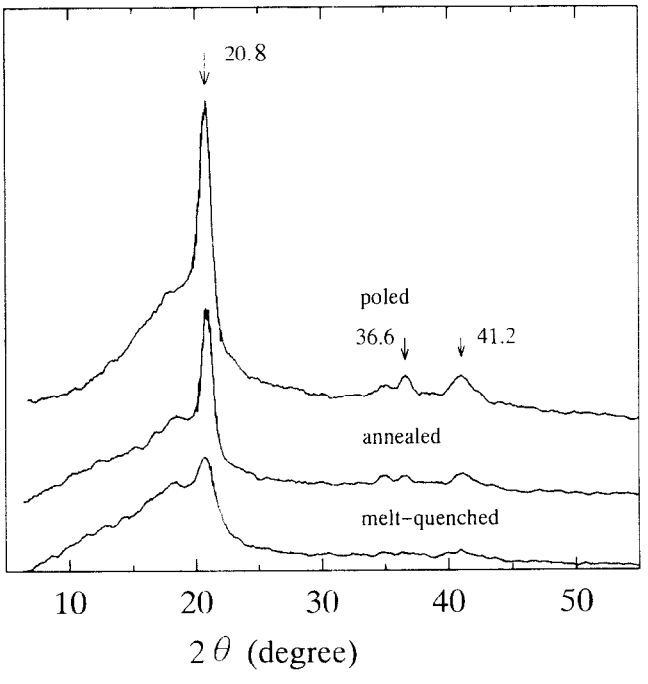

Figure 2 WAXS patterns for the blend samples melt-quenched, thermally annealed and successively poled

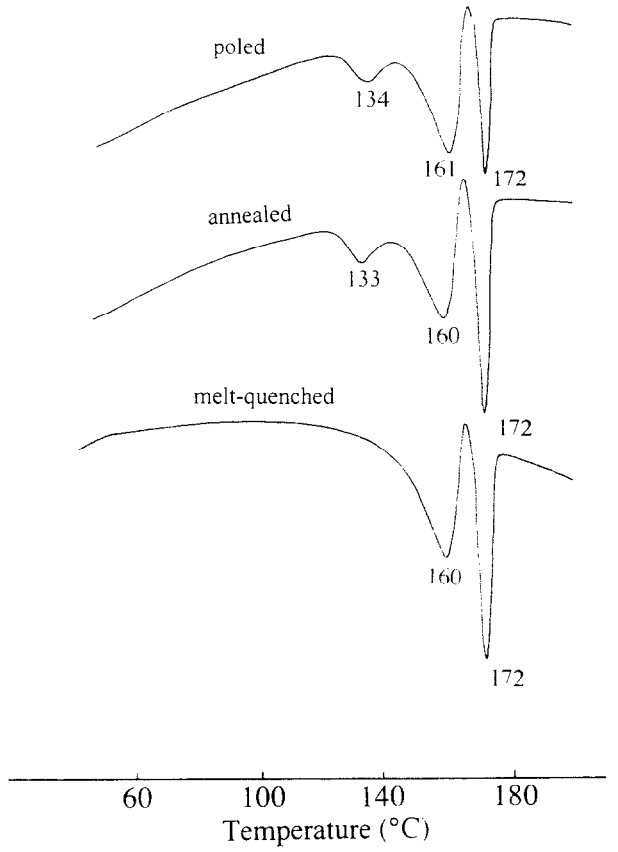

Figure 3 D.s.c. thermograms for the samples corresponding to those in *Figure 2*

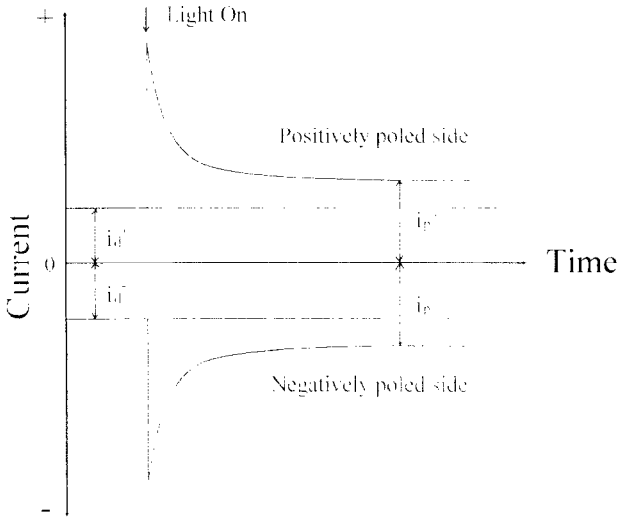

Figure 4 Time–current profile when sample film is illuminated by monochromatic light (timescale: order of 0.5 h)

The current that flowed when the negative poled side is grounded is referred to as i_d^- and i_p^-, with the same definition of subscripts d and p. The dark current may be ascribed to the current due to the carriers thermally generated by the internal electric field. The initial current spike immediately after photo-illumination and the following current decay before it levels out are due mainly to the transient pyroelectric current caused by thermal heating as a result of absorbing the illuminating light, and the pyroelectric response relaxed over a time

extending to the order of 0.5 h. Thus no pyroelectric activity was measured in the current after times longer than about 0.5 h. The value of i_p measured here is the current at longer times (current after thermal relaxation), and I_p determined as $I_p = i_p - i_d$ is the current due only to real photo-activity (real photocurrent). In the case of the unpoled sample, no photocurrent was measured in the entire wavelength region from 250 to 750 nm. The poled PMMA neat sample with PhCz and TNF did not show any significant photo-response. Thus, the fact that only the poled PVDF/PMMA blend sample gave photocurrent activity supports the proposal that the internal electric field created by the preferential alignment of β crystallite dipoles gives rise to significant photo-response current activity. If the counter-charge carriers generated by photo-illumination were to accumulate at the interface between crystallite and amorphous regions and subsequently compensate for polarization in the individual crystallites throughout the sample, one would expect to see the decrease of internal electric field between crystallites and thus the decrease of photocurrent.

Figure 5 shows the dependence of the absolute value of I_p on the wavelength of the illuminating light without applying any external electric field. Open circles denote the photocurrent I_p^+ that flowed when the positive poled side is illuminated, and open triangles denote the photocurrent I_p^- that flowed when the negative poled side is illuminated. The dotted curve in *Figure 5* is the absorption spectrum of PhCz in solution. I_p^+ corresponds to the absorption spectrum of PhCz, while I_p^- has maximum current at around 355 nm, which is the absorption edge of PhCz, and no photocurrent activity in the strong photon absorption region of PhCz below 330 nm. The I_p^+ features in the wavelength region around 330 nm and 270–280 nm are due to the photo-response current via S_1 and S_2 excitation levels, respectively. Both I_p^+ and I_p^- *versus* wavelength profiles indicate that the photons mainly absorbed by PhCz in the positive poled surface generate carriers from the ion-pairs with the assistance of the internal electric field whose vector direction is the same as the poling field. Thus they imply that the photogenerated hole carriers can only be transported among the PhCz hopping sites that resided in the amorphous PVDF/PMMA phase. The 1 wt% content of TNF is too low to allow electron migration among the TNF hopping sites and thus the photocurrent activity in the PhCz absorption region in I_p^- is not measured. If a sufficiently large amount of TNF (for example, the equivalent amount of TNF as PhCz) can be dispersed in the blend, electron migration through TNF would be measured. Further, in this case, the same type of wavelength–photocurrent profile in I_p^- as in the case of I_p^+ would be expected, because the photogenerated electron carriers from the ion-pairs near the negative poled surface can be transported among enough TNF hopping sites to reach the counter positive poled electrode side.

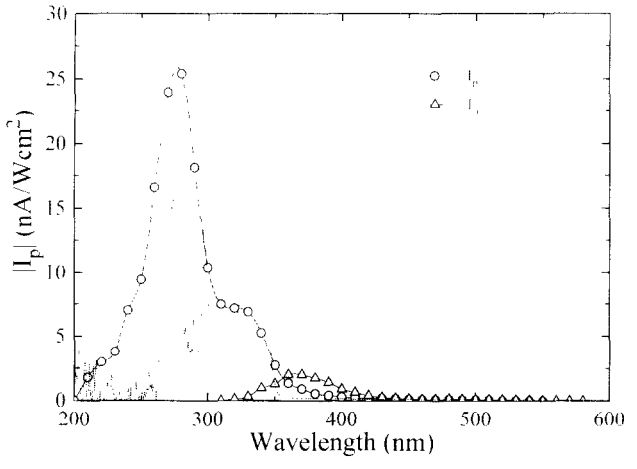

Figure 5 Wavelength dependence of I_p; dotted curve is PhCz absorption spectrum in solution

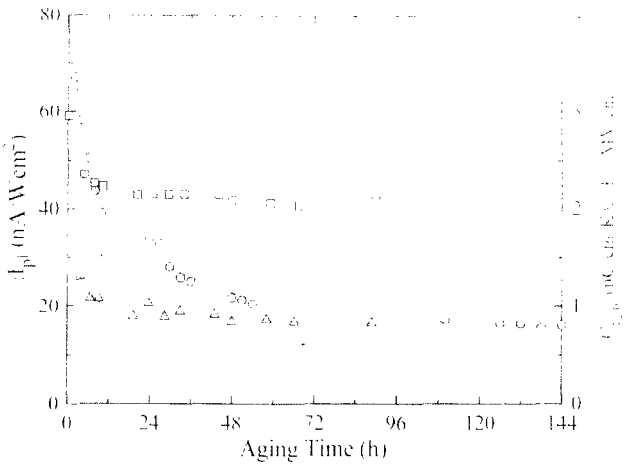

Figure 6 Storage time dependence of I_p (○), E_i (□) and C_{pyro} (△); left vertical scale is for I_p and right vertical scale is for E_i and C_{pyro}; storage temperature is room temperature

A positive external electric field of 6.5 kV cm^{-1} increased I_p^+ by a factor of 2, but a negative external electric field of -6.5 kV cm^{-1} decreased it greatly (photocurrent is too small to be detected). On the contrary, I_p^- increased by a factor of 2 when a negative external electric field was applied, but it decreased to half of the original value when a positive external electric field was applied. The photocurrent–wavelength profiles were not significantly affected by applying either positive or negative external field.

Figure 6 shows the storage time dependence of I_p^+ at 280 nm after poling at 0.5 MV cm^{-1} for 30 min at 80°C. The sample was stored in the dark except for the time spent measuring I_p. The relaxation time of photocurrent decay is essentially the same as those of E_i and C_{pyro} after poling at 0.8 MV cm^{-1} for 1 h shown in the same figure, which were already reported in a previous paper[6]. The decay profiles of photocurrent E_i and C_{pyro} observed are derived from the same nature of the blend samples. The main contribution to these decay trends may be the reorientation or relaxation of the aligned amorphous dipoles at room temperature, which causes the decreases of I_p, C_{pyro} and E_i, whereas the stable state for I_p, C_{pyro} and E_i at longer ageing time is due to the stable aligned crystallite polarization. In the case of present I_p, the poling field is 0.5 MV cm^{-1}, which is close to the coercive field for PVDF β crystallite. Thus the contribution to I_p from amorphous polarization is larger and the relaxation of the aligned amorphous dipoles mainly contributes to the decay of I_p. If the sample is poled at 0.8 MV cm^{-1}, the contribution to I_p from crystallite polarization (E_i due to aligned crystallite dipoles) could be enhanced and

then an I_p decay profile closer to those for E_i and C_{pyro} would be obtained.

Figure 7 shows I_p^+ at 280 nm after the sample film was annealed for 30 min at the fixed temperature shown in the figure. The drastic decrease of I_p^+ in the temperature region above 40°C corresponds well to that for C_{pyro} in the same figure, which was already reported in a previous paper[6]. This drastic decrease of I_p^+ and C_{pyro} is attributed to the relaxation of aligned β-crystallite dipoles above T_g of ca. 40°C. The thermal stability of E_i extending well above T_g up to at least 100°C was explained by the negative space-charge effect injected from the electrode[6]. *Figure 8* shows the wavelength dependence of I_p^+ when the sample is poled at successively higher poling fields. The increase of poling field causes the increase of E_i (ref. 6), which leads to the increase of photocurrent.

Absorption spectra

The pale brown colour of the unpoled sample changed to deep brown after poling under a constant field of 0.7 MV cm^{-1} for 1 h at 80°C. Optical absorption spectra of the samples before and after poling are shown in *Figure 9*. The spectra in the region between 350 and 750 nm confirm this intensity change. It is known that a charge-transfer complex of carbazole derivative and TNF

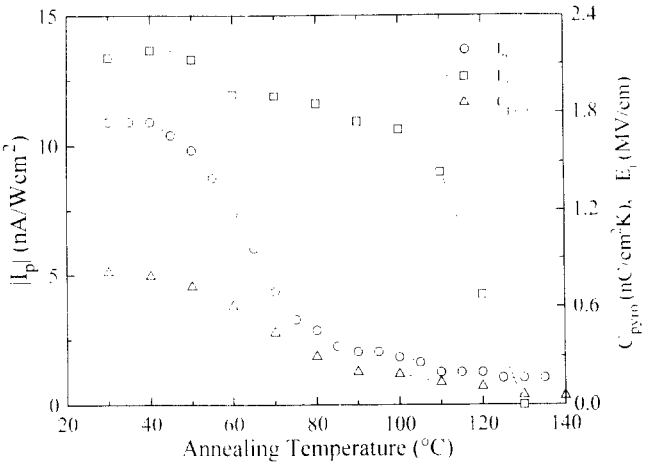

Figure 7 Annealing temperature dependence of I_p (○), E_i (□) and C_{pyro} (△); left vertical scale is for I_r and right vertical scale is for E_i and C_{pyro}

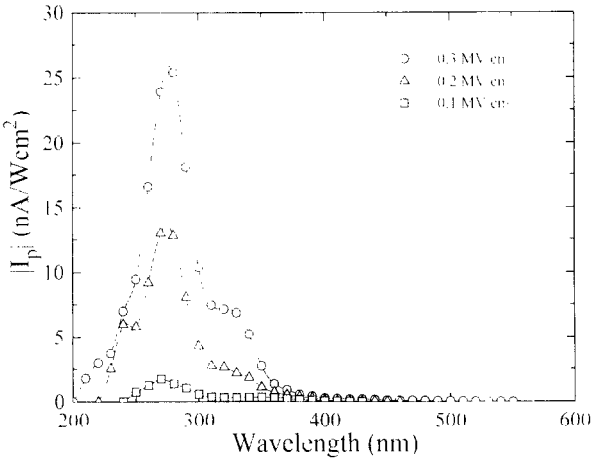

Figure 8 Wavelength dependence of I_p when poling field is increased

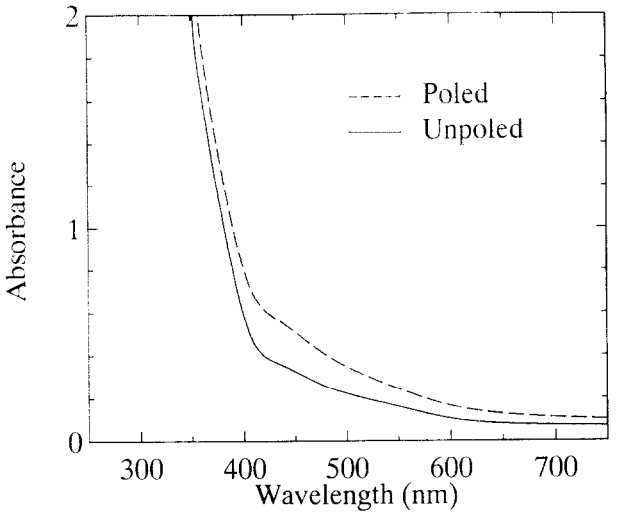

Figure 9 Optical absorption spectra of PhCz–TNF doped PVDF/PMMA blend before and after poling

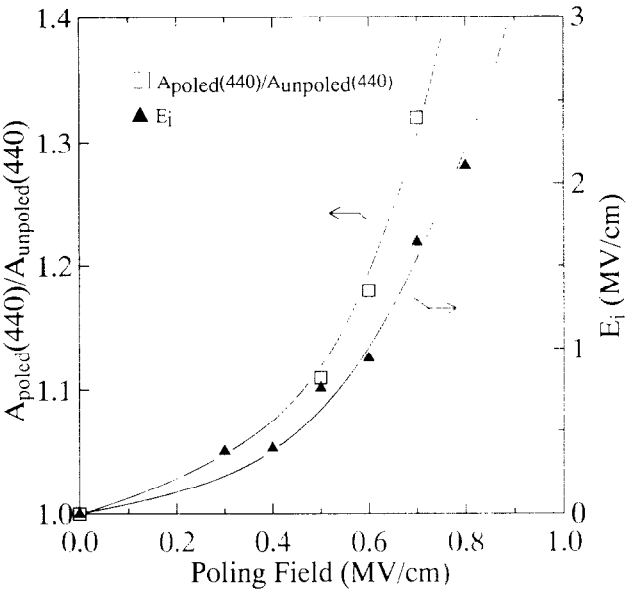

Figure 10 Plots of absorbance ratio at 440 nm between poled and unpoled states and E_i against poling field

gives a broad absorption spectrum extending from 400 nm to over 750 nm and has a peak at around 440 nm. Thus the broad absorption above 400 nm is due to the absorption of the charge-transfer complex between PhCz and TNF. The saturation of absorbance below 350 nm is ascribed to the strong photon absorption by PhCz molecules with large extinction coefficient below 350 nm. *Figure 10* shows the absorption ratio at 440 nm between poled and unpoled states when poling field E_p is increased, corresponding to the increased profile of E_i with E_p previously reported[6]. The non-linear increase of E_i with E_p was shared by that of C_{pyro}[6]. The non-linearity of E_i and C_{pyro} with E_p was explained[6] by the increase in the ratio of crystallite/amorphous polarization with increasing E_p. The non-linear relation of absorption ratio is in good agreement with those of E_i and C_{pyro}. *Figure 11* shows the annealing temperature dependence of absorption ratio at 440 nm and that of E_i, which is the same plot as that in *Figure 7*. The thermal stability of absorption ratio

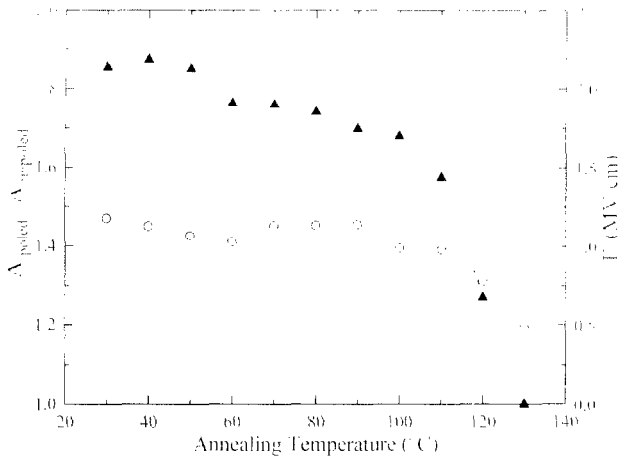

Figure 11 Annealing temperature dependence of absorbance ratio at 440 nm between poled and unpoled states (○) and E_i (▲)

corresponds well to that of E_i. The good correlation between absorption ratio and E_i supports the idea that E_i significantly relates to the electronic state of charge-transfer complex. One explanation for this phenomenon is that the internal electric field induced by the aligned β-crystallite dipoles may enhance the charge-transfer efficiency between PhCz and TNF in the ground state (in other words, total amount of charge-transfer complex is drastically increased by the internal electric field). Another possible explanation is that the vector direction of the dipole moment in the charge-transfer complex may be oriented by the internal electric field.

CONCLUSIONS

The photo-response current induced by the internal electric field created by the preferentially aligned β-crystallite dipoles has been investigated for the blend of PVDF and PMMA. The present system only shows a nanoampere (nA) order photo-response. However, much larger photocurrent will be expected for the case of higher concentration of dispersed PhCz and TNF, which leads to the higher carrier mobility and higher carrier photogeneration.

ACKNOWLEDGEMENTS

This work is supported in part by a Grant-in-Aid for Scientific Research No. 03750649 from the Ministry of Education, Science and Culture, Japan. The authors are sincerely grateful to Dr Saruyama in Kyoto Institute of Technology for the electrometer facility.

REFERENCES

1 Nishi, T. and Wang, T. T. *Macromolecules* 1975, **8**, 909
2 Leonard, C., Halary, J. L., Monnerie, L., Broussoux, D., Servert, B. and Micheron, F. *Polym. Commun.* 1983, **24**, 110
3 Horie, H., Baba, F. and Etoh, S. *Polym. Prepr. Jpn.* 1989, **38**, 3533
4 Tsutsumi, N., Davis, G. T. and DeReggi, A. S. *Macromolecules* 1991, **24**, 6392
5 Tsutsumi, N., Ueda, Y. and Kiyotsukuri, T. *Polym. Commun.* 1992, **33**, 3305
6 Tsutsumi, N., Ueda, Y., Kiyotsukuri, T., DeReggi, A. S. and Davis, G. T. *J. Appl. Phys.* 1993, **74**, 3366
7 Tsutsumi, N., Ono, T. and Kiyotsukuri, T. *Macromolecules* 1993, **26**, 5447
8 Tsutsumi, N., Fujii, I., Ueda, Y. and Kiyotsukuri, T. *Macromolecules* submitted
9 Liptay, W. 'Excited States' (Ed. E. C. Lim.), Academic Press, New York, 1974, Vol. I, pp. 129–229
10 Havinga, E. E. and van Pelt, P. *Ber. Bunsenges. Phys. Chem.* 1979, **83**, 816
11 Czekalla, J. and Wick, G. Z. *Elektrochemie* 1961, **65**, 727
12 Minkin, V. I., Osip, O. A. and Zhdanov, Y. A. 'Dipole Moments in Organic Chemistry', Plenum, New York, 1970, p. 278
13 Davis, G. T., McKinney, J. E., Broadhurst, M. G. and Roth, S. C. *J. Appl. Phys.* 1978, **49**, 4998